

## Expanded View Figures

### Figure EV1. LLOMe treatment alters lysosomal lipid composition.

- A Representative western blot showing purity of immuno-affinity purified lysosomal (LAMP1+) and negative control (IgG Control) treated with 250- $\mu$ M LLOMe for 0, 10 min, and 45 min. Membrane was probed using anti-TOM20 and anti-Calnexin antibodies to verify the absence of mitochondrial and ER membrane, respectively. Enrichment of lysosomes was judged by using an anti-LAMP1 antibody.
- B Numbers of lipid species identified in the produced WCLs and LAMP1+ fraction, belonging to the lipid categories of glycerophospholipids (GPL), sphingolipids (SL), and sterol lipids (ST).
- C Total molar quantities of lipids identified in aliquots of the whole-cell lysates (WCL) produced during lysosome purification.
- D Mol% values of the cardiolipin (CL) and bis(monoacylglycero)phosphate/phosphatidylglycerol (BMP/PG) classes in the LAMP1+ fraction and WCL of untreated HeLa cells. BMP and PG classes are isobaric and reported together as BMP/PG.
- E Enrichment of individual BMP/PG species after purification ( $\log_2$ -transformed fold change, mol% in LAMP1+: mol% in WCL) presented as box plots with individual species as circles, the central band representing the median, the box the upper and lower quartiles, and the whiskers the highest and lowest values. Species are grouped according to the total number of acyl double bonds.
- F Enrichment of monitored lipid classes ( $\log_2$ -transformed fold change, mol% in LAMP1+: mol% in WCL) after purification of lysosomes from untreated cells, presented in a heatmap. The bar plot depicts the percentage of species in the individual classes having positive or negative values of  $\log_2$  fold changes.
- G Representative mass spectra of three PtdInsP species. Precursor ions detected in the MS1 and their theoretical  $m/z$  values (MS1) and MS2 spectra obtained after their fragmentations, displaying the relative intensities of the ions.

Data information: Bars and error bars denote mean  $\pm$  SD from  $n = 3$ –4 independently performed purifications. Multiple t-tests were performed to assess changes between means of pmol (C) and mol% values and  $\log_2$ -transformed mol% values (D–F). Resultant  $P$ -values were corrected for multiple testing using Benjamini–Hochberg correction and differences were considered statistically significantly changed with adjusted  $P$ -values ( $q$ -values) of 0.05 or less. \* $q < 0.05$ ; \*\* $q < 0.01$ . Abbreviations: FA, fatty acid; glycerolP, glycerol phosphate; InsP, phosphorylinositol headgroup. Additional abbreviations are as in Fig 1.

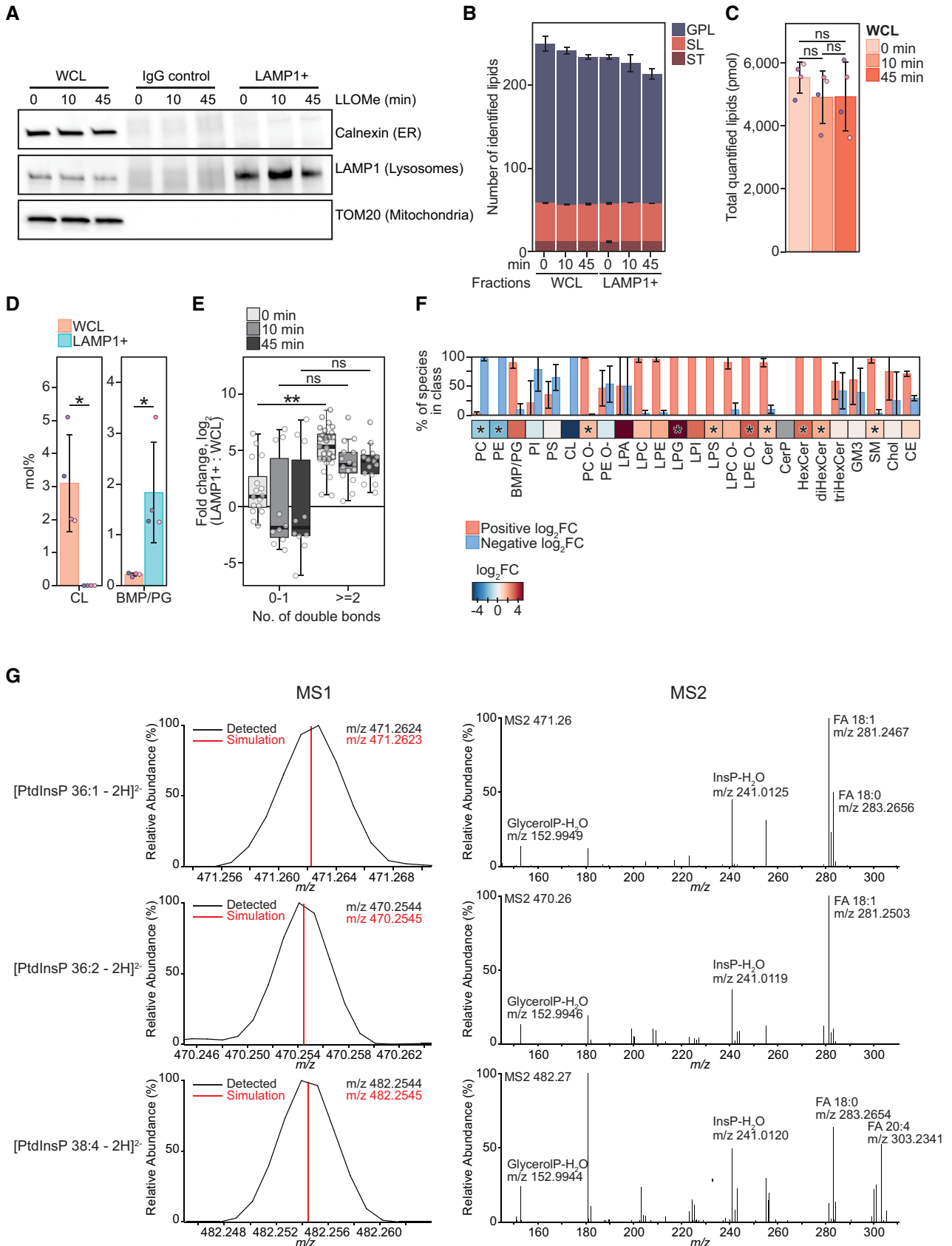


Figure EV1.

**Figure EV2. Mol% of lipid classes in whole-cell lysates (WCL) and purified lysosomes (LAMP1+ fractions).**

Mol% of all monitored lipid classes in the WCLs and LAMP1+ fractions from cells untreated or treated with LLOMe for 10 or 45 min.

Data information: Bars and error bars denote mean  $\pm$  SD from  $n = 3-4$  independently performed purifications. Multiple  $t$ -tests were performed to assess changes between means. Resultant  $P$ -values were corrected for multiple testing using Benjamini–Hochberg correction and differences were considered statistically significantly changed with adjusted  $P$ -values ( $q$ -values) of 0.05 or less. \* $q < 0.05$ . Abbreviations are as in Fig 1.

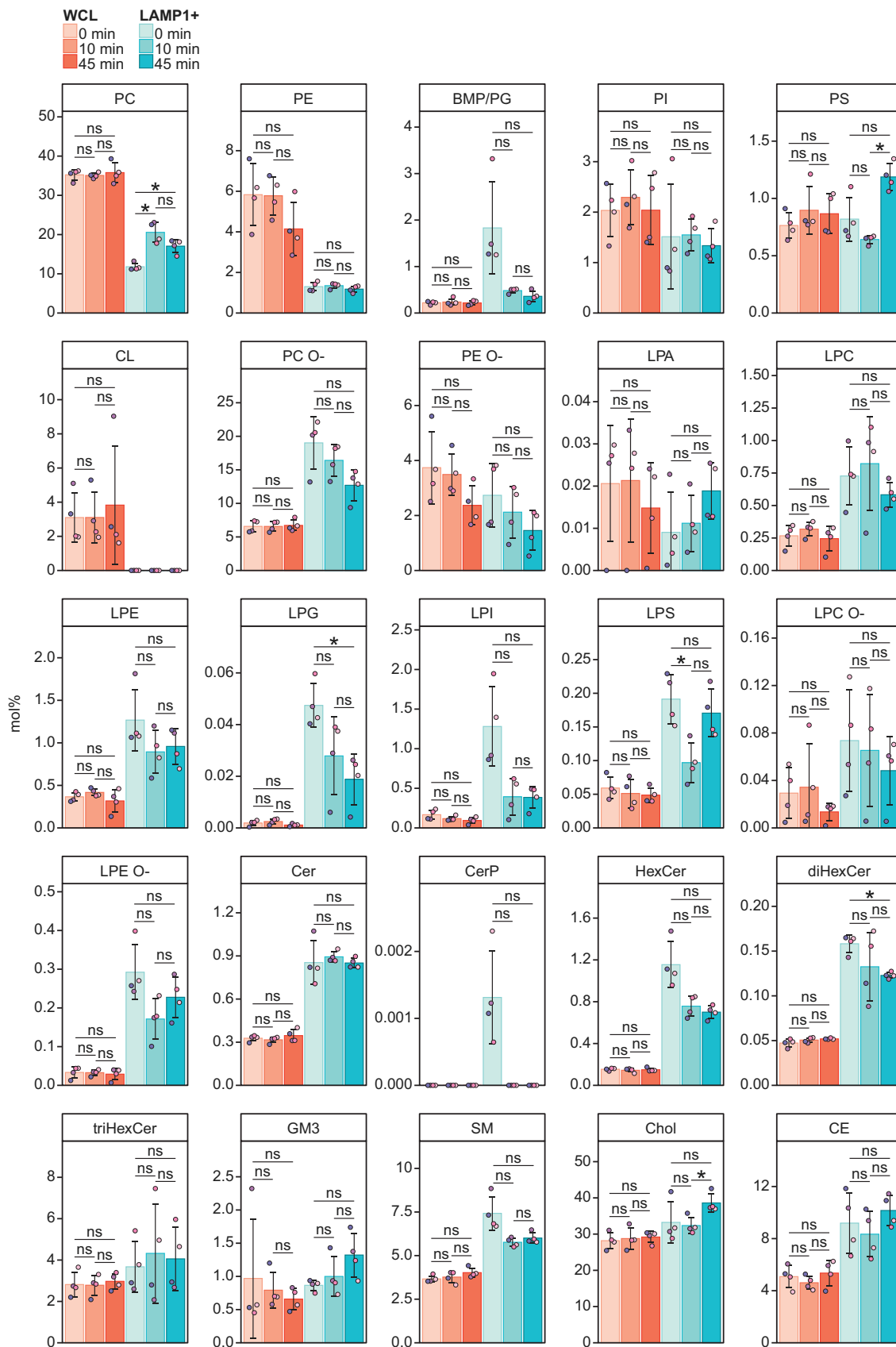


Figure EV2.

**Figure EV3. Mean total numbers of double bonds in whole-cell lysates (WCLs) and purified lysosomal fractions (LAMP1+ fractions).**

Mean total numbers of double bonds in the monitored lipid classes in the WCLs and LAMP1+ fractions from cells untreated or treated with LLOMe for 10 or 45 min. The double bonds are in the acyl (alkyl) groups of glycerophospholipids and sterol lipids, and in the acyl group and long-chain base groups of sphingolipids.

Data information: Bars and error bars denote mean  $\pm$  SD from  $n = 3-4$  independently performed purifications. Multiple t-tests were performed to assess changes between means. Resultant  $P$ -values were corrected for multiple testing using Benjamini–Hochberg correction and differences were considered statistically significantly changed with adjusted  $P$ -values ( $q$ -values) of 0.05 or less. \* $q < 0.05$ ; \*\* $q < 0.01$ ; \*\*\* $q < 0.001$ . Abbreviations are as in Fig 1.

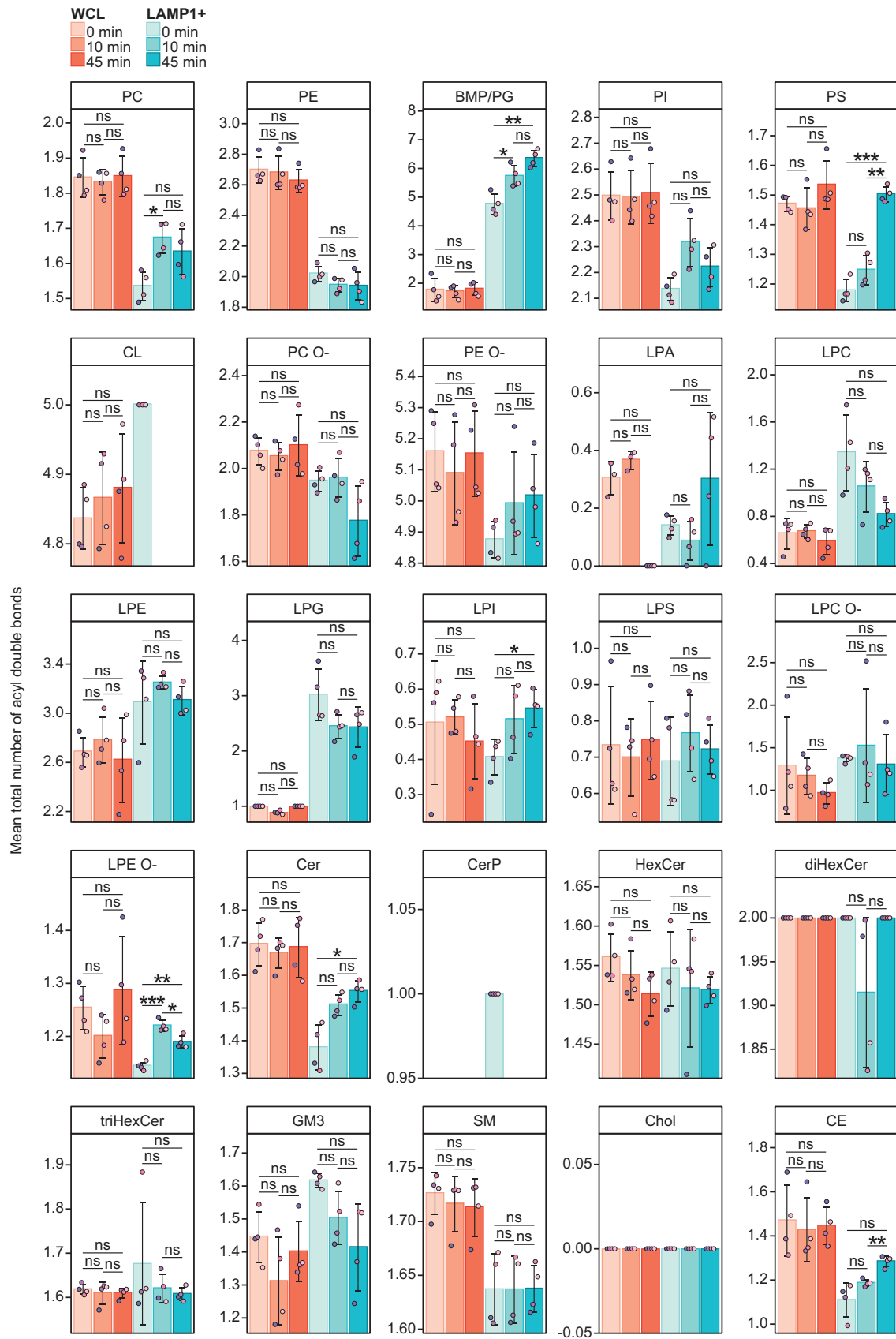


Figure EV3.

**Figure EV4. A targeted mini-screen for recruitment of phosphoinositides to damaged lysosomes.**

Representative movie montages of live-cell imaging experiments using mCherry-tagged lipid probes in HeLa cells stably expressing CHMP4B-eGFP. P40PX was used for the detection of PtdIns3P, SidM for the detection of PtdIns4P, mL1N for the detection of PtdIns(3,5)P<sub>2</sub>, and PLCδ-PH for the detection of PtdIns(4,5)P<sub>2</sub>. CHMP4B-eGFP was used as a positive control for lysosomal damage. Scale bar: 5 μm.

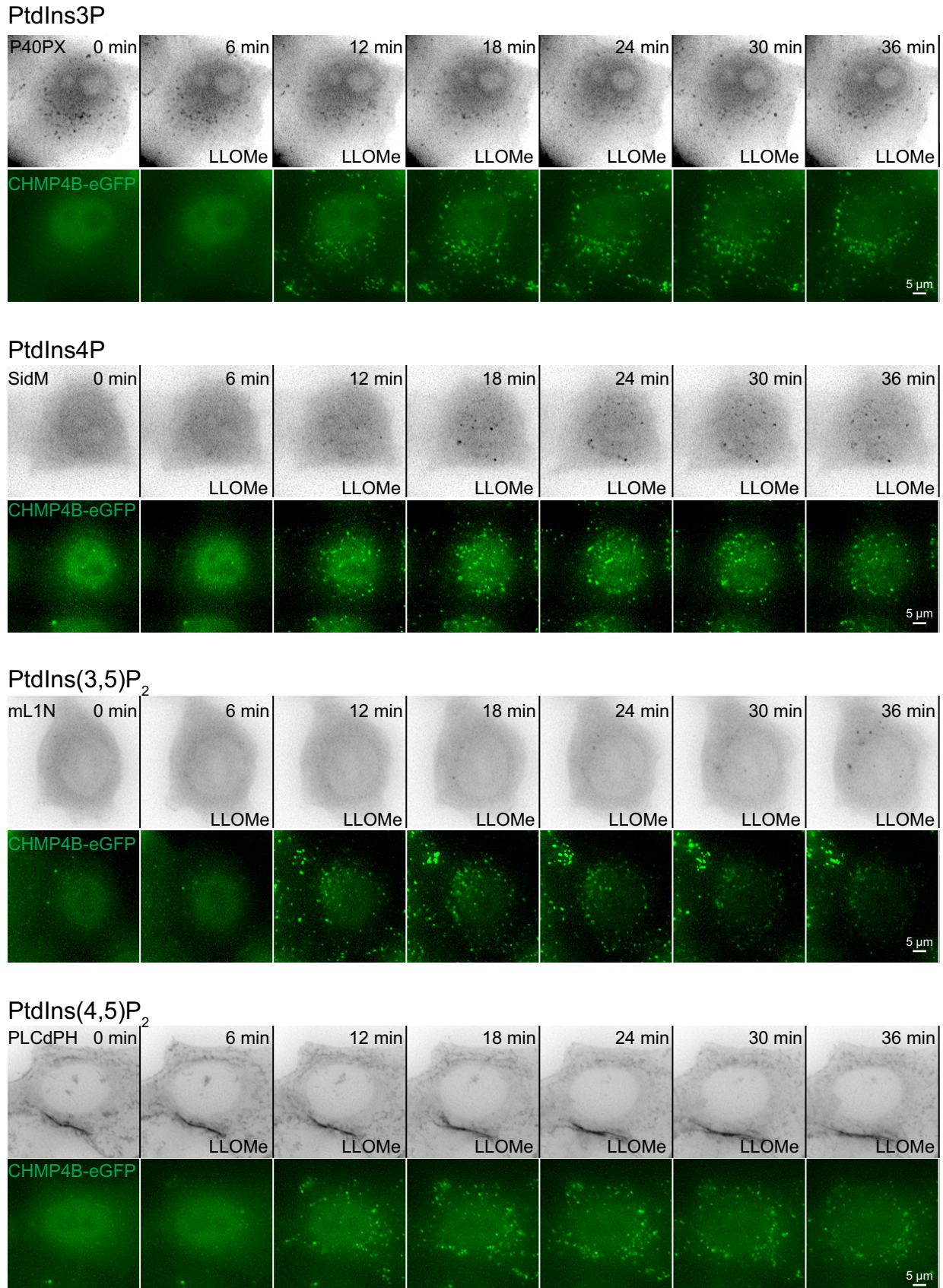
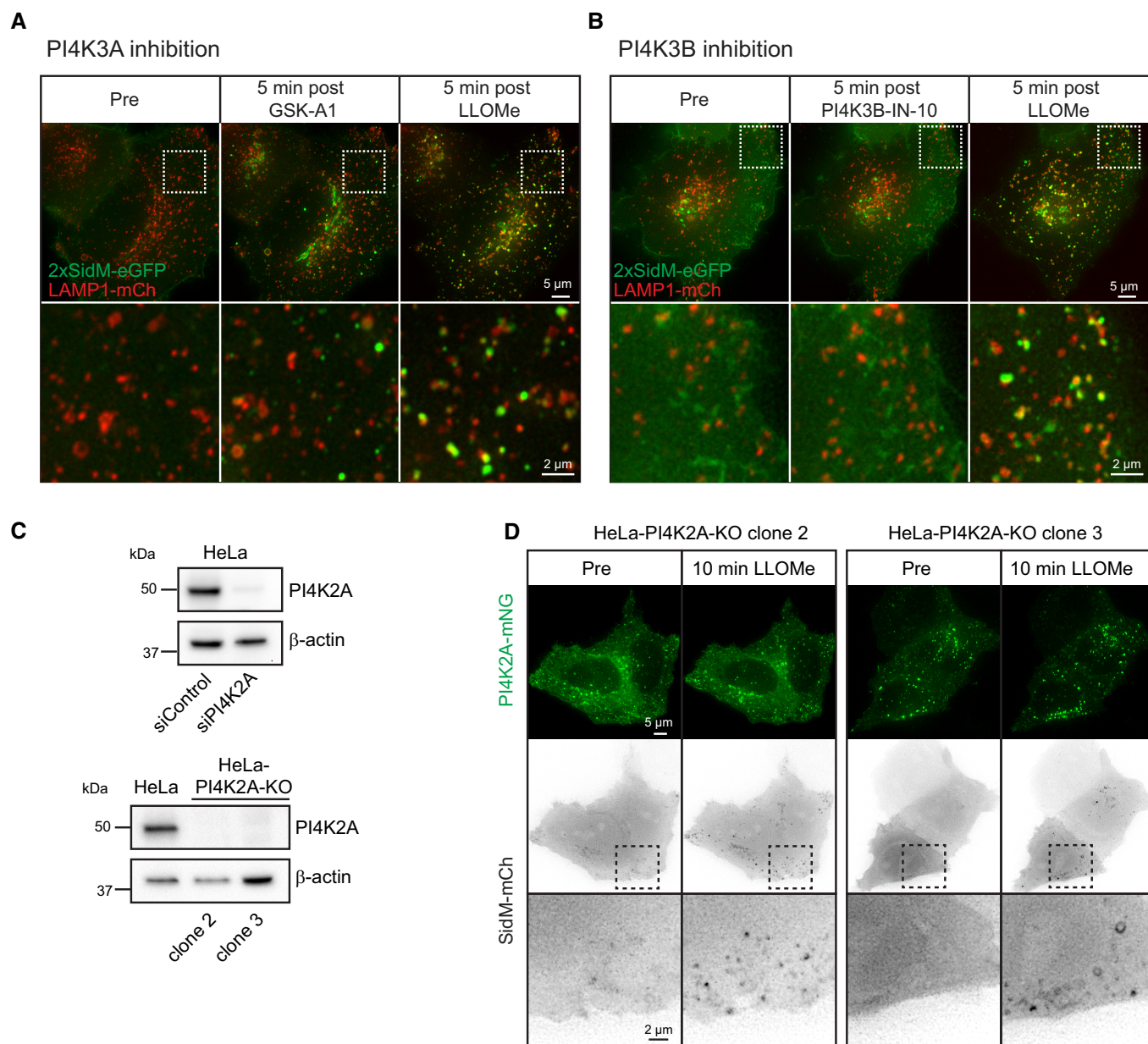


Figure EV4.

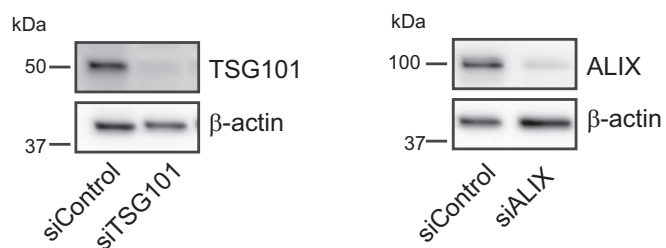




**Figure EV5. PI4K3A and PI4K3B do not mediate PtdIns4P recruitment at damaged lysosomes.**

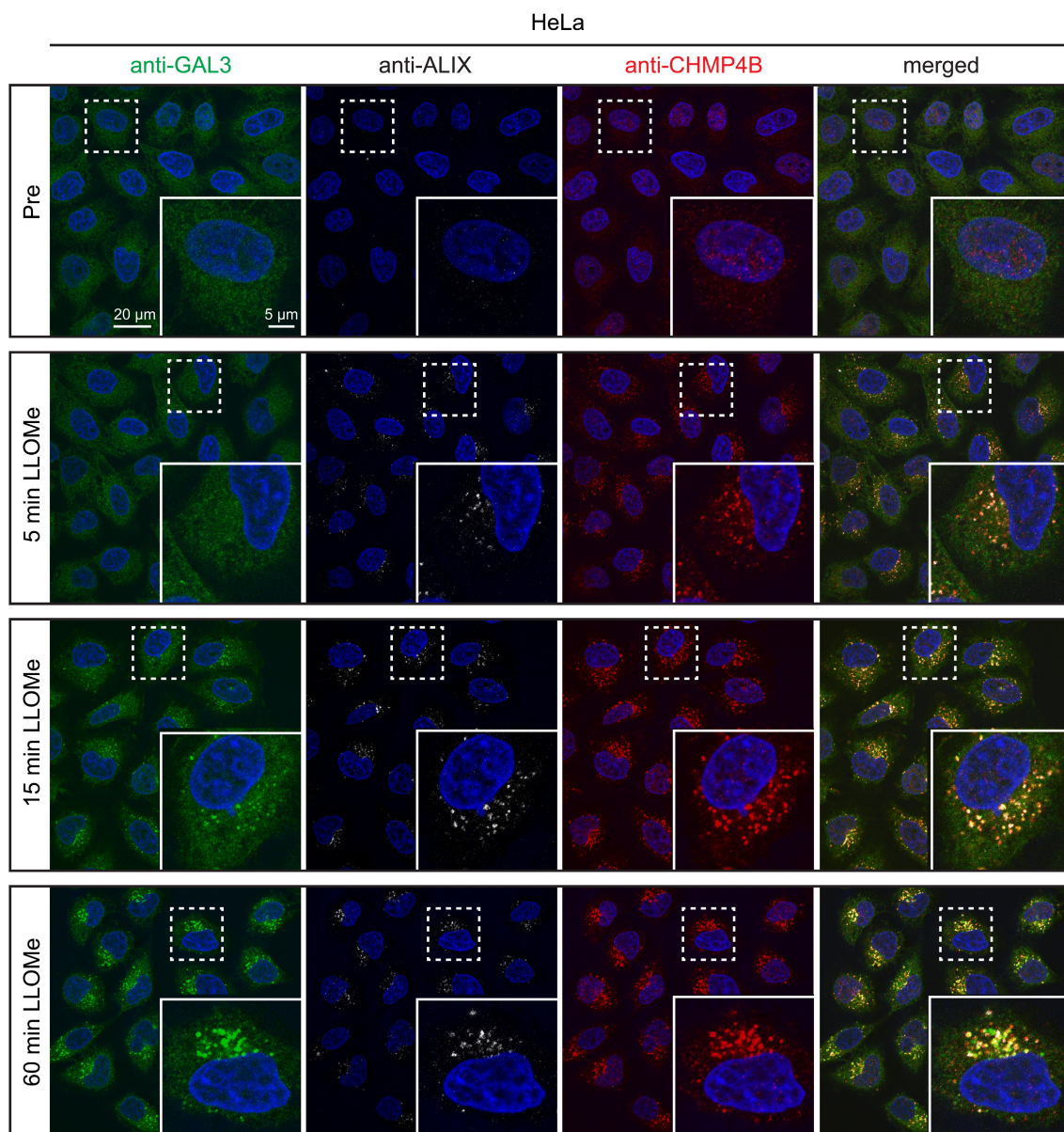
- A Movie stills from live-cell imaging experiments of HeLa cells transiently expressing the PtdIns4P probe 2xSidM-eGFP and the lysosomal marker LAMP1-mCherry. Cells were incubated with 10-nM PI4K3A inhibitor GSK-A1 for approximately 16 min before 250- $\mu$ M LLOMe was added.
- B Movie stills from live-cell imaging experiments of HeLa cells transiently expressing the PtdIns4P probe 2xSidM-eGFP and the lysosomal marker LAMP1-mCherry. Cells were incubated with 25-nM PI4K3B inhibitor PI4K3B-IN-10 for approximately 30 min before 250- $\mu$ M LLOMe was added.
- C Knockdown efficiency of siRNA against PI4K2A or CRISPR-Cas9-mediated knockout of PI4K2A (clone 2 and clone 3) as detected by western blot using an anti-PI4K2A antibody.  $\beta$ -actin used as a loading control.
- D Exogenous expression of PI4K2A-mNG and the PtdIns4P probe SidM-mCherry in clone 2 and clone 3 of PI4K2A-KO cells shows recruitment of SidM-mCherry after incubation with 250- $\mu$ M LLOMe.

Source data are available online for this figure.

**Figure EV6. Knockdown efficiency of TSG101 or ALIX.**

Knockdown efficiency of siRNA oligonucleotides for TSG101 or ALIX as detected by western blot using anti-TSG101 or anti-ALIX antibodies.  $\beta$ -actin used as a loading control.

Source data are available online for this figure.

**Figure EV7. ESCRT and GAL3 recruitment to damaged lysosomes.**

Representative fluorescence micrographs of parental HeLa cells treated with 250- $\mu$ M LLOMe or an equal volume of DMSO (Pre) for 5 min, 15 min, and 1 h before fixation and immunostained with Hoechst (blue), anti-CHMP4B (red), anti-GAL3 (green), and anti-ALIX (white) (Fig 5B).